

## Investigation of the Binding Determinants of Phosphopeptides Targeted to the Src Homology 2 Domain of the Signal Transducer and Activator of Transcription 3. Development of a High-Affinity Peptide Inhibitor

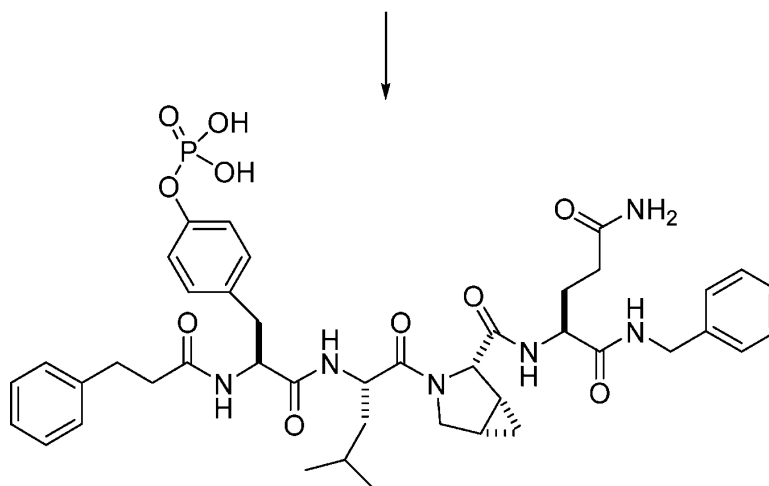
Coleman, Zhiyong Ren, Pijus K. Mandal, Arlin G. Cameron, Garrett A. Dyer, Seema Muranjan, Martin Campbell, Xiaomin Chen, and John S. McMurray

*J. Med. Chem.*, **2005**, 48 (21), 6661-6670 • DOI: 10.1021/jm050513m • Publication Date (Web): 16 September 2005

Downloaded from <http://pubs.acs.org> on March 29, 2009

Ac-Tyr-Leu-Pro-Gln-Thr-Val-NH<sub>2</sub>

**1**, IC<sub>50</sub> = 290 nM



**50**, IC<sub>50</sub> = 125 nM

### More About This Article

Additional resources and features associated with this article are available within the HTML version:

- Supporting Information
- Links to the 15 articles that cite this article, as of the time of this article download
- Access to high resolution figures
- Links to articles and content related to this article



# Journal of Medicinal Chemistry

Subscriber access provided by American Chemical Society

- Copyright permission to reproduce figures and/or text from this article

[View the Full Text HTML](#)



**ACS Publications**  
High quality. High impact.

Journal of Medicinal Chemistry is published by the American Chemical Society, 1155  
Sixteenth Street N.W., Washington, DC 20036

## Investigation of the Binding Determinants of Phosphopeptides Targeted to the Src Homology 2 Domain of the Signal Transducer and Activator of Transcription 3. Development of a High-Affinity Peptide Inhibitor

David R. Coleman, IV,<sup>†,‡</sup> Zhiyong Ren,<sup>‡,§</sup> Pijus K. Mandal,<sup>†</sup> Arlin G. Cameron,<sup>†</sup> Garrett A. Dyer,<sup>†</sup> Seema Muranjan,<sup>†</sup> Martin Campbell,<sup>#</sup> Xiaomin Chen,<sup>§</sup> and John S. McMurray<sup>\*,†</sup>

Department of Neuro-Oncology, Department of Biochemistry and Molecular Biology, Department of Molecular Pathology, and The Graduate School of Biomedical Sciences, The University of Texas M. D. Anderson Cancer Center, 1515 Holcombe Boulevard, Houston, Texas 77030

Received June 1, 2005

Signal transducer and activator of transcription 3 (Stat3) is a cytosolic transcription factor that relates signals from the cell membrane directly to the nucleus where it, in complex with other proteins, initiates the transcription of antiapoptotic and cell cycling genes, e.g., Bcl-x<sub>L</sub> and cyclin D1. In normal cells Stat3 transduces signals from cytokines such as IL-6 and growth factors such as the epidermal growth factor. Stat3 is constitutively activated in a number of human tumors. Antisense and dominant negative gene delivery result in apoptosis and reduced cell growth, thus this protein is an attractive target for anticancer drug design. As part of our research on the design of Src homology 2 (SH2) directed peptidomimetic inhibitors of Stat3, in this paper we describe structure–activity relationship studies that provide information on the nature of peptide–protein interactions of a high-affinity phosphopeptide inhibitor of Stat3 dimerization and DNA binding, Ac-Tyr(PO<sub>3</sub>H<sub>2</sub>)-Leu-Pro-Gln-Thr-Val-NH<sub>2</sub>, peptide **1**. There is a hydrophobic surface on the SH2 domain that can accommodate lipophilic groups on the N-terminus. Of the amino acids tested, leucine provided the highest affinity at pY+1 and its main chain NH is involved with a hydrogen bond with Stat3, presumably Ser636. *cis*-3,4-Methanoproline is optimal as a backbone constraint at pY+2. The side chain amide protons of Gln are required for high-affinity interactions. The C-terminal dipeptide, Thr-Val, can be replaced with groups ranging in size from methyl to benzyl. We synthesized a phosphopeptide incorporating groups that provided increases in affinity at each position. Thus, hydrocinnamoyl-Tyr(PO<sub>3</sub>H<sub>2</sub>)-Leu-*cis*-3,4-methanoPro-Gln-NHBn, **50**, was the highest affinity peptide, exhibiting an IC<sub>50</sub> of 125 nM versus 290 nM for peptide **1** in a fluorescence polarization assay.

Signal transducer and activator of transcription 3 (Stat3) is a member of the signal transducer and activator of transcription (STAT) family of transcription factors that relate signals from extracellular signaling protein receptors on the plasma membrane directly to the nucleus (reviewed in refs 1a–c). Stat3 was discovered as a major component in the acute phase response to inflammation<sup>2</sup> and a key mediator of interleukin 6 (IL-6) and epidermal growth factor signaling.<sup>3</sup> Like all STATs, Stat3 is composed of an amino-terminal oligomerization domain, a coiled coil domain, a DNA binding domain, a linker domain, an Src homology 2 (SH2) domain, and a C-terminal transactivation domain. On binding of IL-6 to its receptor, JAK kinases-2 (JAK-2) phosphorylates the coreceptor gp130 on several tyrosines.<sup>4,5</sup> Stat3, via its SH2 domain, binds to these phosphotyrosine residues. It is then phosphorylated on Tyr705, a conserved tyrosine just C-terminal to the SH2 domain, by JAK-2. Upon phosphorylation, termed activation, Stat3 forms homodimers (and/or heterodimers with Stat1) via reciprocal interactions between the SH2

domains and pTyr705. The dimers then translocate to the nucleus and bind specific DNA sequences where they, in cooperation with other transcription factors, regulate gene expression.<sup>1</sup> Downstream targets of Stat3 include Bcl-x<sub>L</sub>, a member of the Bcl-2 family of antiapoptotic proteins, cell cycle regulators such as cyclin D1 and p21<sup>WAF1/CIP1</sup>, and other transcription factors including c-myc and c-fos. In epidermal growth factor (EGF) signaling, Stat3 has been reported to bind directly to phosphotyrosine residues on the epidermal growth factor receptor (EGFR) and to be activated by the kinase activity of the receptor.<sup>6</sup> Further studies imply that Src kinases first bind to EGFR via their SH2 domains and recruit Stat3 via SH3 domain interactions with polyproline helices.<sup>7</sup>

Stat3 has been shown to be constitutively activated in cancers of the head and neck,<sup>8</sup> breast,<sup>9</sup> brain,<sup>10</sup> prostate,<sup>11</sup> lung,<sup>12</sup> leukemia,<sup>13</sup> multiple myeloma,<sup>14</sup> lymphoma,<sup>15</sup> pancreas,<sup>16</sup> and others.<sup>17</sup> Inhibition of Stat3 activity by the introduction of antisense oligonucleotides or dominant negative constructs has been shown to induce apoptosis and reduce cell growth and soft agar colony formation in several tumor cell lines exhibiting constitutively active Stat3.<sup>14,18</sup> In those cells driven by EGF signaling, introduction of small-molecule EGFR inhibitors reduced Stat3 activation and resulted in cell

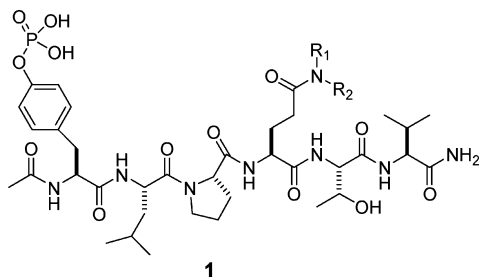
\* To whom correspondence should be addressed. Phone: 713-745-3763. Fax: 713-834-6230. E-mail: jsmcmur@mdanderson.org.

<sup>†</sup> Department of Neuro-Oncology.

<sup>‡</sup> The Graduate School of Biomedical Sciences.

<sup>§</sup> Department of Biochemistry and Molecular Biology.

<sup>#</sup> Department of Molecular Pathology.

**Chart 1.** Structure of Peptide 1, Ac-Tyr(PO<sub>3</sub>H<sub>2</sub>)-Leu-Pro-Gln-Thr-Val-NH<sub>2</sub>

death.<sup>19</sup> A small-molecule inhibitor of the Src kinase also inhibits Stat3 activation, induces apoptosis, and inhibits cell growth in a breast cancer cell line.<sup>20</sup> Thus Stat3 is an attractive target for cancer drug design.<sup>17</sup>

To develop inhibitors capable of inhibiting Stat3 activity, we are targeting the SH2 domain with a phosphopeptide-based peptidomimetic approach.<sup>21</sup> Such compounds are expected to block the binding of Stat3 to cytokine or growth factor receptors and thereby prevent phosphorylation, dimerization, and nuclear translocation. For dimerized Stat3, SH2-directed inhibitors would also inhibit dimerization and DNA binding, thereby reducing the expression of antiapoptosis and cell cycling genes. SH2 domains are specific for phosphotyrosine-containing amino acid sequences with specificity for individual proteins residing C-terminal to this residue.<sup>22,23</sup> Phosphopeptides based on the sequence surrounding phosphotyrosine-705 of Stat3,<sup>24–26</sup> EGFR,<sup>26,27</sup> and gp130<sup>26</sup> were shown to inhibit dimerization and DNA binding in electrophoretic mobility shift assays (EMSA). To find a lead peptide, we screened a series of phosphopeptides derived from the amino acid sequences of receptor docking sites of Stat3 for their ability to inhibit dimer formation and DNA binding using EMSA.<sup>26</sup> Sequences from Stat3, gp130, EGFR, IL-10R, and GM-CSF were tested. Of this group, Ac-Tyr(PO<sub>3</sub>H<sub>2</sub>)-Leu-Pro-Gln-Thr-Val-NH<sub>2</sub> (**1**, Chart 1) was found to be the most potent inhibitor (IC<sub>50</sub> = 150 nM) and was selected as the lead compound. Peptide **1** is composed of residues 904–909 of gp130, the cocomponent of the IL-6 receptor, and possesses the consensus sequence for Stat3 binding, Tyr(PO<sub>3</sub>H<sub>2</sub>)-Xxx-Xxx-Gln reported by Stahl et al.<sup>4</sup> and Gerhartz et al.<sup>5</sup> Truncation and alanine scanning experiments showed that the C-terminal valine was not necessary for binding, leucine at pY+1 contributed to affinity, proline was necessary for high-affinity activity, and glutamine was essential for binding.<sup>26</sup> Similar to other SH2 domains,<sup>28</sup> Stat3 ligands bind in a (pY)–(pY+3) “two-pronged” motif.

SH2 domain inhibitor development efforts against Src, Grb2, and others have relied on X-ray crystallographic or NMR-derived structures to provide understanding of peptide–protein interactions and to guide the conversion of peptide into non-peptide. The crystal structure of the dimer of Stat3 $\beta$  bound to DNA<sup>29</sup> reveals the interactions between the phosphopeptide segment Tyr(PO<sub>3</sub>H<sub>2</sub>)/705-Leu-Lys-Thr-Lys-Phe of one protein molecule and the SH2 domain of the other (Figure 1). The phosphate is in contact with the side chains of Lys591 ( $\alpha$ A2), Arg609 ( $\beta$ B5), Ser611 ( $\beta$ B7), and Ser613 (BC2) and the main chain NH of Glu612 (BC1) in a manner nearly identical with that of phosphopeptide complexes

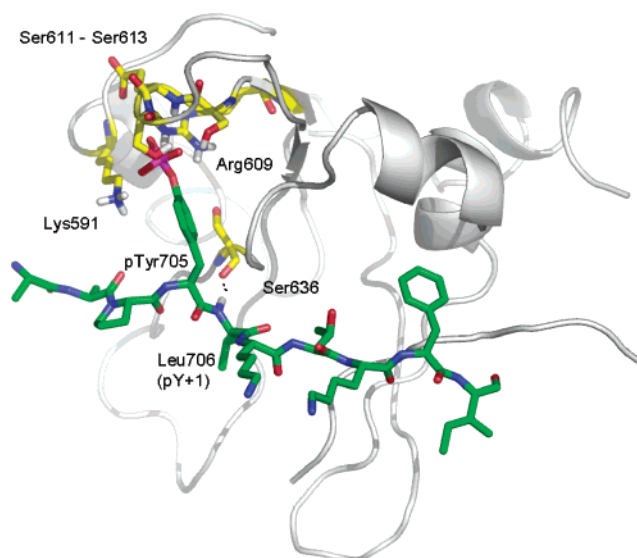


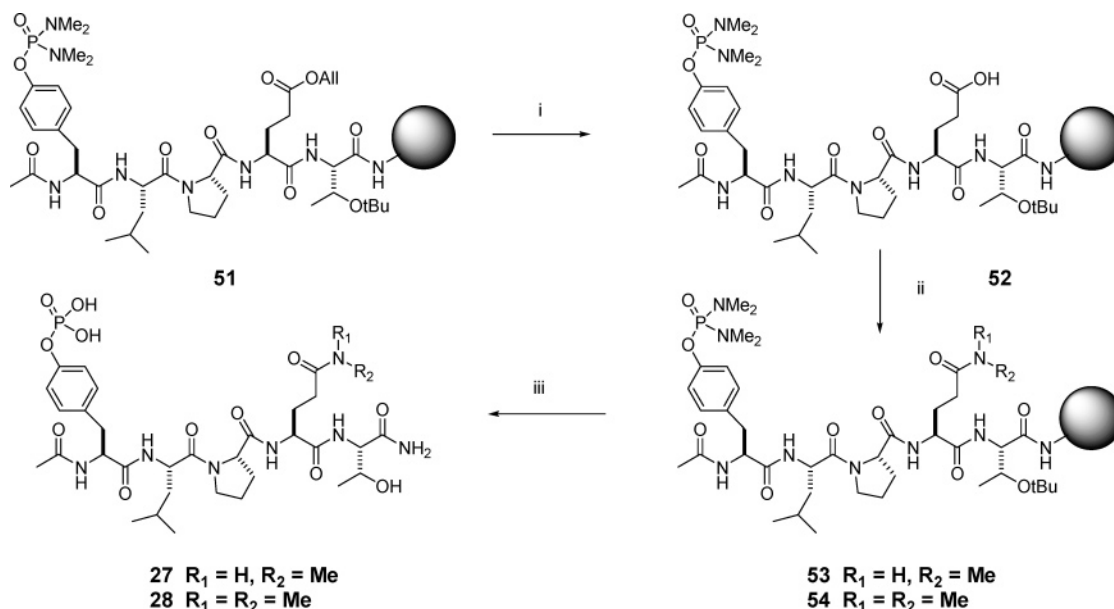
**Figure 1.** Structure of the phosphopeptide, residues 702–711 (green), of Stat3 bound to the SH2 domain of the opposing protein in the Stat3 $\beta$  dimer/DNA complex.<sup>29</sup> Phosphotyrosine705 interacts with the side chains of Lys591, Arg609, Ser611, and Ser613 and the main chain NH of Glu612 (yellow). The hydrogen bond between the  $\alpha$ NH of Leu706 and the backbone C=O of Ser636 on the opposing protein is depicted as a dotted line. Coordinates were kindly provided by C. Mueller.<sup>29</sup> They can be obtained from the Protein Data Bank, entry 1BG1. Figure was generated using PyMol.<sup>48</sup>

of Src,<sup>28,30a,b</sup> Grb2,<sup>30c</sup> Lck,<sup>30d</sup> p85 PI3K,<sup>30e,f</sup> Stat1,<sup>31</sup> and others. A hydrogen bond exists between the  $\alpha$ NH of Leu706 and the C=O of Ser636 ( $\beta$ D2) on the opposing protein. Similar interactions are noted between the pY+1 residue of phosphopeptide ligands and the  $\beta$ D4 residue of other SH2 domains. (The architecture of Stat3 is somewhat different from the other signaling proteins, hence the variation in the designation of the  $\beta$ D2 and  $\beta$ D4 residues.) Thus, the pY and pY+1 residues in the Stat3 dimer bind similarly to analogous residues in other SH2 domains. However, the X-ray structure does not provide a direct model of the interaction of the Pro-Gln-Thr-Val residues of peptide **1** and Stat3. Therefore, SAR studies were undertaken to further understand the contributions to affinity of backbone and side chain groups of our lead peptide.<sup>32</sup>

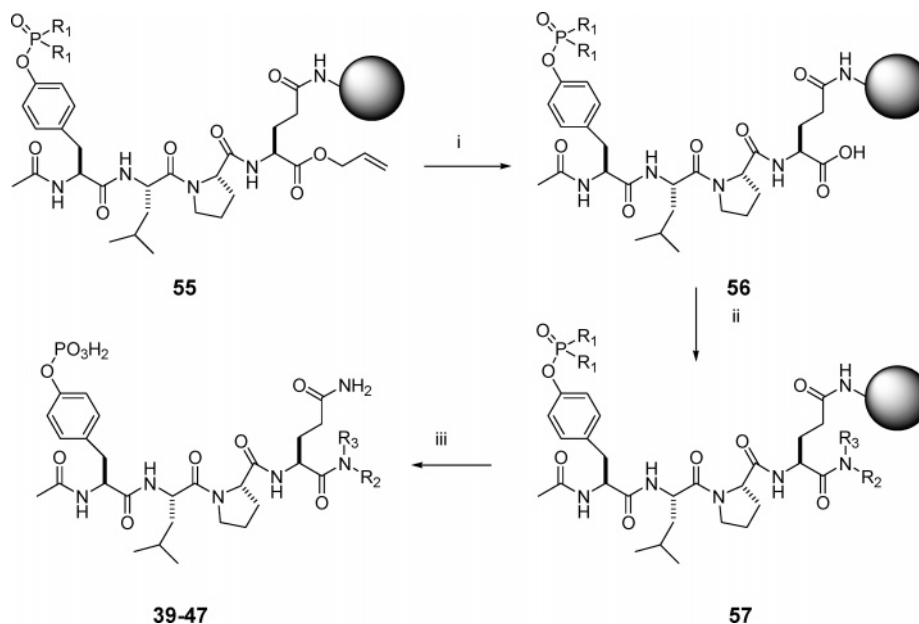
## Chemistry

Phosphopeptides were synthesized using either manual or automated solid-phase methods using the Fmoc protection scheme and carbodiimide/HOBt or PyBOP/HOBt/DIPEA coupling techniques. Unless otherwise noted, phosphotyrosine was introduced as the unprotected phosphate<sup>33</sup> using PyBOP/HOBt/DIPEA coupling conditions. The amino termini were capped with excess acetic anhydride and Et<sub>3</sub>N. Peptides were cleaved with TFA/TIS/H<sub>2</sub>O, 95:2.5:2.5,<sup>34</sup> and purified by reverse-phase HPLC before assay.

**Methylation of the Side Chain Amide of Gln.** The synthesis of Ac-Tyr(PO<sub>3</sub>H<sub>2</sub>)-Leu-Pro-Glu(NR<sub>1</sub>R<sub>2</sub>)-Thr-NH<sub>2</sub> (**27**, **28**) is depicted in Scheme 1. Ac-Tyr(PO-[NMe<sub>2</sub>]<sub>2</sub>)-Leu-Pro-Glu(OAll)-Thr(tBu) (**51**) was synthesized on Rink amide resin using automated protocols. The allyl group on the side chain of glutamic acid was removed with tetrakis(triphenyl)phosphine/palladium in

**Scheme 1.** Synthesis of Methylated Glutamine-Containing Peptides<sup>a</sup>

<sup>a</sup> Reagents and conditions: (i)  $[Ph_3P]_4Pd$ , NMM, AcOH; (ii) amine, PyBOP, DIPEA, HOBt; (iii) (a) TFA/TIS/ $H_2O$ , 1 h, (b) 10%  $H_2O$ /TFA, overnight.

**Scheme 2.** Synthesis of Ac-Tyr( $PO_3H_2$ )-Leu-Pro-Gln-Xxx<sup>a</sup>

<sup>a</sup> Reagents and conditions: (i)  $[Ph_3P]_4Pd$ , NMM, AcOH; (ii) amine, PyBOP, DIPEA, HOBt; (iii) (a) TFA/TIS/ $H_2O$ , 1 h, (b) 10%  $H_2O$ /TFA, overnight.

the presence of acetic acid and *N*-methylmorpholine.<sup>35</sup> Derivatization of the carboxyl group was carried out by the addition of 5 equiv of  $NH_2Me$  or  $NHMe_2$  with PyBOP/HOBt/DIPEA (**53**, **54**). The use of phosphotyrosine with unprotected phosphate<sup>33</sup> or protected with diphenylmethylsilylethyl groups<sup>36</sup> resulted in poor yields and very impure products. Replacement of the phosphate group on the tyrosine with bis(dimethylamino)-phosphoramidate<sup>37</sup> resulted in better quality crude products. Conversion of the phosphoramidate to the phosphate requires aqueous acidic conditions.<sup>37</sup> So after cleavage from the resin, 10%  $H_2O$  was added and acidolysis was allowed to proceed overnight. It was also found that the Dmb protection on the side chain of Glu, with removal with 2% hydrazine in DMF,<sup>38</sup> resulted in

unacceptable levels of side products that were not there with the allyl/ $Pd[0]$  protecting group scheme.

**C-Terminal Derivatization.** To synthesize tetrapeptides in which the C-terminal Thr was replaced (**39–47**), Ac-Tyr( $PO[NMe_2]_2$ )-Leu-Pro-Glu-OAll (**55**) was assembled using automated methods starting with attachment of the side chain of Fmoc-Glu-OAll to Rink resin (Scheme 2). The allyl group was cleaved using  $(PPh_3)_4Pd$ /AcOH/NMM<sup>35</sup> to give the free carboxyl group of the C-terminal Gln (**56**). The amines were added in excess, and coupling was mediated with DIPCDI/HOBt to minimize racemization (**57**). TFA cleavage gave the desired peptides, **39–47**, which were purified by reverse-phase HPLC. As above, use of nonprotected phosphotyrosine resulted in crude peptides of low purity.



Coupling of pyrrolidine was incomplete, and the resulting tetrapeptide, Ac-Tyr(PO<sub>3</sub>H<sub>2</sub>)-Leu-Pro-Gln-OH (**43**), was obtained and assayed.

Peptides **31**, **32**, and **34–38**, in which Gln was replaced by Gaba or cyclic amino acids, were synthesized by coupling commercially available Fmoc-protected amino acids to Rink amide resin using manual solid-phase peptide synthesis. For the synthesis of **38**, Fmoc-pyrrolidine-3-carboxylic acid, **58**, was prepared by standard coupling of Fmoc-OSu to commercially available pyrrolidine-3-carboxylic acid under aqueous alkaline conditions. The final peptide, hydrocinnamoyl-Tyr(PO<sub>3</sub>H<sub>2</sub>)-Leu-3,4-*cis*-methanoPro-Gln-NHBn (isomers **49** and **50**), was synthesized by manual solid-phase peptide synthesis. Fmoc-Glu-NHBn, **59**, was attached to Rink amide resin via the side chain carboxyl group using PyBOP/HOBt/DIPEA coupling methodology. The remainder of the residues were coupled in the same manner. The final product consisted of two diastereomers that were readily resolvable by reverse-phase HPLC using a gradient of MeOH in 0.01 M NH<sub>4</sub>OAc, **49** and **50**. Fmoc-Glu-NHBn (**59**) was prepared by coupling benzylamine to commercially available Fmoc-Glu(OtBu)-OH using water-soluble carbodiimide followed by removal of the side chain *tert*-butyl group with TFA.

## Results

Haan et al.<sup>39</sup> assayed several phosphopeptides based on gp130 and LIFR as well as the sequence surrounding Stat3 Tyr705 for binding to the isolated SH2 domain from Stat3. At pH 7.5 no complex formation was observed, whereas binding occurred at pH 5.5. It was noted that at the higher pH the SH2 domain existed in a dimerized state, which may have precluded phosphopeptide binding. Binding constants determined at pH 5.5 must be considered tenuous because the conformation of the protein may be altered by the acidic environment. Therefore, full length Stat3 was used to assay our compounds. This protein was not phosphorylated on Tyr705 prior to use.

For the SAR studies reported here, peptides were assayed for competition of a fluorescently tagged version of our lead peptide using fluorescence polarization (FP).<sup>40</sup> Thus, Ala-Tyr(PO<sub>3</sub>H<sub>2</sub>)-Leu-Pro-Gln-Thr-Val-NH<sub>2</sub> was labeled at the amino terminus with the isomeric mixture fluorescein-5(6) carboxylic acid. Synthesis of this probe produced two isomers, and the second compound to elute by reverse-phase HPLC was found to bind to Stat3 with higher affinity (data not shown). The individual 5- and 6-carboxyfluorescein isomers were purchased and coupled to the N-terminus of Ala-Tyr(PO<sub>3</sub>H<sub>2</sub>)-Leu-Pro-Gln-Thr-Val-NH<sub>2</sub>. The peptide capped with 5-carboxyfluorescein coeluted with the high-affinity isomer on reverse-phase HPLC. Thus, the probe used for FP was 5-carboxyfluoresceinyl-Ala-Tyr(PO<sub>3</sub>H<sub>2</sub>)-Leu-Pro-Gln-Thr-Val-NH<sub>2</sub>. Subsequent batches of probe were synthesized with the 5-isomer. In FP titration assays, the bacterially expressed protein was identical to that expressed in the baculovirus-Sf9 system employed for our earlier study<sup>24,26</sup> when assayed by FP (data not shown).

The initial screen phosphopeptides based on known receptor docking sites for Stat3 was done using electro-

**Table 1.** IC<sub>50</sub> Values of Peptide Inhibitors of Stat3

peptide	IC <sub>50</sub> (nM)	
	EMSA <sup>a</sup>	FP
<b>1</b> Ac-Tyr(PO <sub>3</sub> H <sub>2</sub> )-Leu-Pro-Gln-Thr-Val-NH <sub>2</sub>	150	290 ± 63
<b>2</b> Ac-Tyr(PO <sub>3</sub> H <sub>2</sub> )-Leu-Pro-Gln-Thr-NH <sub>2</sub>	600	739 ± 31
<b>3</b> Ac-Tyr(PO <sub>3</sub> H <sub>2</sub> )-Leu-Pro-Gln-NH <sub>2</sub>	1000	856 ± 41

<sup>a</sup> IC<sub>50</sub> values from ref 26.

**Table 2.** Amino Terminal Substitutions in Peptide 2

peptide	R	IC <sub>50</sub> (μM)
<b>2</b>	Ac	0.739 ± 0.031
<b>4</b>	PhCO	0.814 ± 0.078
<b>5</b>	CH <sub>3</sub> CH <sub>2</sub> CO	0.497 ± 0.010
<b>6</b>	PhCH <sub>2</sub> OCO	0.750 ± 0.072
<b>7</b>	PhCH <sub>2</sub> CH <sub>2</sub> CO	0.276 ± 0.012

phoretic mobility shift assays.<sup>26</sup> Peptide **1** and C-terminal truncated peptides **2** and **3** were reassayed using fluorescence polarization. The IC<sub>50</sub> values obtained by both methods followed the same trend of decreasing affinity with decreasing length, although the values varied somewhat (Table 1). Thus, the C-terminal residues play a role in binding.

The peptides used in this study were analogues of peptide **2**. The C-terminal of Val in **1** was removed to increase synthesis efficiency and to simplify interpretation of the results.

**Amino-Terminal Substitutions.** To test for potential binding affinity not afforded by the amino-terminal acetyl group of our lead peptide, a small survey of acyl groups was conducted at pY-1 (Table 2). Of the groups tested, the propionyl and hydrocinnamoyl groups (**5** and **7**) exhibited increases in affinity. Interestingly, the benzyloxycarbonyl group (Cbz) of **6** did not change the apparent affinity. The Cbz and hydrocinnamoyl groups are isosteric. The gain in affinity due to the hydrocinnamoyl group of **7** was offset by the α-oxygen atom in the Cbz group. During their studies of phosphopeptide inhibitors based on the Stat3 Tyr705 sequence, Turkson et al.<sup>25</sup> noted no significant difference in affinity in peptides with a proline or an alanine that is just amino-terminal to the phosphotyrosine (position pY-1). However, significant changes were observed when substituted benzoyl groups or 3-pyridinecarbonyl groups were employed in a series of dipeptides of the structure Xxx-Tyr(PO<sub>3</sub>H<sub>2</sub>)-Leu.<sup>41</sup> Taken together with our results, it appears that there is a hydrophobic patch on the surface of Stat3 SH2 domain that is just amino-terminal to the Tyr(PO<sub>3</sub>H<sub>2</sub>) binding pocket.

**Substitutions at pY+1.** In the crystal structure of dimerized Stat3β dimer bound to DNA, the side chain of Leu706 at the pY+1 position of Tyr(PO<sub>3</sub>H<sub>2</sub>)/705-Leu-Lys-Thr-Lys-Phe resides on a nonpolar surface of the opposing SH2 domain. A survey of hydrophobic amino acids was conducted to find which would provide optimum binding (Table 3, peptides **8–13**). The β-substituted residues, Val and Ile, decreased activity. In-

**Table 3.** Inhibition of Stat3 with Analogues of **2** Substituted at Position pY+1: Ac-Tyr(PO<sub>3</sub>H<sub>2</sub>)-Xxx-Pro-Gln-Thr-NH<sub>2</sub>

peptide	pY+1	IC <sub>50</sub> (μM)
<b>2</b>	Leu	0.739 ± 0.031
<b>8</b>	Val	1.54 ± 0.079
<b>9</b>	Ile	1.07 ± 0.059
<b>10</b>	Phe	1.89 ± 0.20
<b>11</b>	Cha	0.91 ± 0.12
<b>12</b>	Nle	0.717 ± 0.080
<b>13</b>	Ph <sub>2</sub> Ala	> 100
<b>14</b>	NMe-Leu	> 100

terestingly, Phe was 2-fold less active than the fully reduced analogue cyclohexylalanine. Nle resulted in activity closest to that of Leu. Diphenylalanine resulted in an inactive compound.

As mentioned, the Leu706 NH at pY+1 participates in a hydrogen-bond interaction with the backbone carbonyl of Ser636 of the opposing protein (Figure 1). Replacement of the Leu amide proton with a methyl group would preclude formation of this hydrogen bond and would also sterically prevent tight association of the peptide with the protein surface. Incorporation of *N*-methylleucine at pY+1, peptide **14**, destroyed activity of the peptide (IC<sub>50</sub> > 100 μM). Thus, it seems likely that the Leu residue of our peptide binds similarly to the pY+1 residues found in the Stat3 crystal structure<sup>29</sup> and other SH2 domain ligands.<sup>28,30,31</sup>

**Substitutions at pY+2.** Our initial screen of receptor docking sites and the alanine scan established that proline at position pY+2 is very important for affinity.<sup>26</sup> This amino acid experiences no rotation about the Nα-Cα bond, which may be important in constraining the peptide to a population of conformations resembling the bound conformation. To further probe structural effects at pY+2, cyclic amino acids were substituted for proline (Table 4).

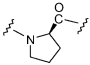
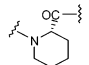
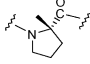
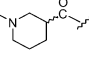
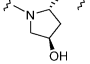
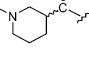
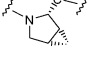
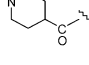
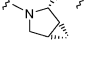
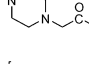
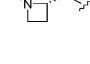
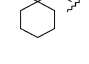
Not surprisingly, the *D*-amino acid (**15**) severely curtailed binding. α-Methyl substitution reduced activity 3- to 4-fold (**16**). 4-Hydroxyproline (**17**) resulted in a slight increase in affinity. Incorporation of *cis*-3,4-methanoproline resulted in two peptides that were readily separable by reverse-phase HPLC and that gave

the correct molecular mass (**18**, **19**). The first eluting isomer (**18**) enhanced affinity of the peptide 2-fold (IC<sub>50</sub> = 0.265 μM), and the second (**19**) reduced affinity (IC<sub>50</sub> = 3.11 μM). Fmoc-*cis*-3,4-methanoproline is sold as a racemic mixture of (2*S*,3*R*,4*S*)- and (2*R*,3*S*,4*R*)-enantiomers. Thus, **18** and **19** are diastereomers.

The homologous cyclic amino acids, four-membered azetidine-2-carboxylate and six-membered pipercolic acid, resulted in lower affinity peptides (**20** and **21**, respectively). The structural isomers of pipercolic acid nipecotic acid (Nip) and isonipecotic acid (Inp) were also incorporated. Moving the position of the carbonyl group from the α- to the β- (Nip) or the γ-carbon (Inp) alters the spatial the relationship of the glutamine to the rest of the peptide, most importantly tyrosine. Nip was obtained commercially as a racemic mixture of the *R* and *S* isomers. During purification by preparative HPLC, we were able to isolate the two diastereomers of Ac-Tyr(PO<sub>3</sub>H<sub>2</sub>)-Leu-(*R,S*)-Nip-Gln-Thr-NH<sub>2</sub> (peptides **22** and **23**), though we do not know which contains the *R* or *S* isomer. Both exhibited a 50-fold reduction in affinity, as did the peptide containing Inp (**24**). 4-Carboxymethylpiperazine (Cmpi) was also substituted for proline, and the resulting peptide, **25**, was very weak (IC<sub>50</sub> = 57.1 μM). The unnatural amino acid analogue, α-aminocyclohexane carboxylic acid (1-Ac<sub>6</sub>C), was reported to be a substitute for proline and to induce a β-turn or a 3<sub>10</sub> helix.<sup>42</sup> It was incorporated into Grb2 SH2 domain antagonists to induce a β-turn at pY+1.<sup>43</sup> In peptide **26**, 1-Ac<sub>6</sub>C resulted in a 20-fold reduction in affinity, suggesting that the peptide may not bind to Stat3 in a turn structure. Thus, *cis*-methanoproline is the scaffold that provides the optimum disposition of contact groups for interaction with Stat3.

**Gln Side Chain Amide Protons Are Required for High-Affinity Interaction with Stat3.** Glutamine at position pY+3 was found early to be a binding determinant for the Stat3 SH2 domain,<sup>4,5</sup> and most known receptor docking sites for Stat3 possess the consensus sequence Tyr-Xxx-Xxx-Gln.<sup>4,5,26,44</sup> This was confirmed in our screening of receptor docking sites<sup>26</sup> and by screening of a combinatorial phosphopeptide library<sup>45</sup>

**Table 4.** Inhibition of Stat3 with Analogues of **2** Substituted at Position pY+2: Ac-Tyr(PO<sub>3</sub>H<sub>2</sub>)-Leu-Xxx-Gln-Thr-NH<sub>2</sub>

Peptide	Pro Analogue	Xxx	IC <sub>50</sub> (μM)	Peptide	Pro Analogue	Xxx	IC <sub>50</sub> (μM)
<b>15</b>	D-Pro		>100	<b>21</b>	Pipercolic acid		1.24 ± 0.078
<b>16</b>	α-Methyl-Pro		1.87 ± 0.162	<b>22</b>	Nipecotic acid-1		38.6 ± 0.259
<b>17</b>	<i>trans</i> -4-hydroxy-Pro		0.484 ± 0.019	<b>23</b>	Nipecotic acid-2		33.1 ± 1.79
<b>18</b>	<i>cis</i> -3,4-methanoPro-1		0.265 ± 0.014	<b>24</b>	Isonipecotic acid		34.6 ± 1.16
<b>19</b>	<i>cis</i> -3,4-methanoPro-2		3.11 ± 0.110	<b>25</b>	Piperazine-1-acetic acid		57.1 ± 8.09
<b>20</b>	Azetidine-2-carboxylic acid		1.66 ± 0.079	<b>26</b>	1-Amino-1-carboxycyclo-hexane		13.4 ± 0.396

**Table 5.** Effect of Modifications of the Side Chain of Gln in Ac-Tyr(PO<sub>3</sub>H<sub>2</sub>)-Leu-Pro-XXX-Thr-NH<sub>2</sub>

peptide	pY+3	IC <sub>50</sub> (μM)
<b>2</b>	Gln	0.739 ± 0.031
<b>27</b>	Gln(Me)	18.1 ± 2.60
<b>28</b>	Gln(Me <sub>2</sub> )	80.0 ± 15.0
<b>29</b>	Met(O)	9.87 ± 1.36
<b>30</b>	Met(O <sub>2</sub> )	13.9 ± 0.72

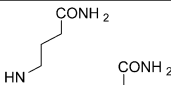
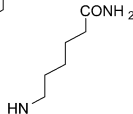
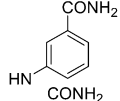
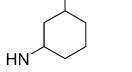
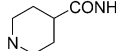
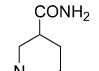
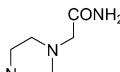
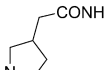
for Stat3 ligands. Previously we found that glutamic acid at pY+3 abrogated activity and that asparagine attenuated activity.<sup>26</sup> The side chain amide protons could serve as H-bond donors, either in intermolecular interactions or in an intramolecular manner in conformations resembling the bound state prior to binding. To determine the role of these protons, one or both were substituted with methyl groups. With the goal of membrane permeability in mind, these substitutions, if tolerated, would serve to make the peptide more hydrophobic, thus enhancing biological activity. Substitution of one of the side chain amide protons reduced binding by 25-fold (**27**, Table 5, IC<sub>50</sub> = 18 μM). Addition of a second methyl group brought the IC<sub>50</sub> to 80 μM (peptide **28**). The reduction in affinity may be due to loss of important inter- or intramolecular hydrogen bonding, steric crowding in a binding pocket accommodating the Gln side chain, or both. Thus, these amide protons are required for affinity.

The role of the Gln carbonyl oxygen was probed by substitution of methionine sulfoxide and methionine sulfone, peptides **29** and **30**, respectively. In both cases inhibition was curtailed 20- to 30-fold (Table 5). Methionine sulfoxide is isosteric with Gln; the sulfonyl group mimics the side chain carbonyl, and the methyl group replaces the NH<sub>2</sub>. The fact that Met(O) resulted in a dramatic loss of inhibition underscores the contribution of the carboxamide NH<sub>2</sub> group on the side chain of the pY+3 residue. However, the retention of modest activity suggests that the carbonyl group may also be involved in intermolecular interactions.

**Substitutions at pY+3.** Glutamine can be considered to be  $\gamma$ -carboxy- $\gamma$ -aminobutyric acid ( $\gamma$ -carboxy-Gaba). To test the effect of the main chain carboxamide, glutamine was substituted with 4-aminobutyramide (peptide **31**) and was compared to peptide **3**. As shown in Table 6 this substitution reduced affinity 2-fold (IC<sub>50</sub> = 1.8 μM). Thus, the main chain carboxamide of Gln enhances activity by inter- or intramolecular interactions. The Gaba homologue,  $\epsilon$ -aminohexanoic acid amide (Ahx), further decreased inhibition (peptide **32**).

Gln was substituted with nonpeptidic, cyclic amino acid amides to constrain the rotation of the side chain (Table 6). 3-Carboxamidoaniline is a highly constrained mimic in which the carboxamido group is spaced from the proline carbonyl by the same number of atoms as Gln, but all atoms are coplanar. Peptide **33** was 45-fold less active than peptide **3**, suggesting that in the bound state the Gln side chain is not coplanar. The saturated analogue aminocyclohexane-3-carboxamide (3Ac<sub>6</sub>c-NH<sub>2</sub>) resulted in approximately 4-fold higher affinity than the aniline mimic, IC<sub>50</sub> = 9.81 μM for **34** versus IC<sub>50</sub> = 36 μM for **33**. However, 3Ac<sub>6</sub>c-NH<sub>2</sub> resulted in a 10-fold reduction in affinity relative to peptide **3**. Interestingly, nipecotamide, piperazine-1-acetamide, and pyrrolidine-1-acetamide (peptides **35**, **37**, and **38**, respectively),

**Table 6.** Effect of Gln Mimics in the Peptide Ac-Tyr(PO<sub>3</sub>H<sub>2</sub>)-Leu-Pro-XXX

Peptide	Gln Analogue	XXX	IC <sub>50</sub> (μM)
<b>31</b>	Gaba		1.78 ± 0.132
<b>32</b>	Ahx		9.78 ± 2.02
<b>33</b>	3-Carboxamidoaniline		36.6 ± 2.63
<b>34</b>	3-Ac <sub>6</sub> c-NH <sub>2</sub>		9.81 ± 1.14
<b>35</b>	Nipecotamide		3.02 ± 0.811
<b>36</b>	Isonipecotamide		11.8 ± 1.19
<b>37</b>	Piperazine-1-acetamide		1.40 ± 0.50
<b>38</b>	Pyrrolidine-3-acetamide		1.69 ± 0.057

**Table 7.** Affinities of Peptides with the Structure Ac-Tyr(PO<sub>3</sub>H<sub>2</sub>)-Leu-Pro-Gln-R

peptide	R	IC <sub>50</sub> (μM)
<b>3</b>	NH <sub>2</sub>	0.856 ± 0.041
<b>39</b>	NHMe	0.882 ± 0.077
<b>40</b>	NHBn	0.409 ± 0.015
<b>41</b>	NHCH(Me)Ph ( <i>S</i> )	0.596 ± 0.082
<b>42</b>	NHCH(Me)Ph ( <i>R</i> )	0.801 ± 0.142
<b>43</b>	OH	0.748 ± 0.085
<b>44</b>	NMe <sub>2</sub>	1.85 ± 0.675
<b>45</b>	NEt <sub>2</sub>	4.22 ± 0.074
<b>46</b>	pyrrolidine	2.11 ± 0.401
<b>47</b>	piperidine	7.00 ± 0.988
<b>48</b>	<i>N</i> -methyl-Thr-NH <sub>2</sub>	1.22 ± 0.051

possessing endocyclic “backbone” nitrogens, decreased activity by only 2- to 4-fold compared to peptide **3**. This reduced activity may be due to the lack of the “main chain” NH proton from the Gln surrogate or from a slightly imperfect fit. Isonipecotamide reduced activity 14-fold (**36**).

**Substitutions at pY+4.** Tetrapeptides were prepared in which the C-terminal Thr of **2** was replaced with non-amino-acid groups (Table 7). This was done to determine (1) the necessity of the pY+4 residue and (2) if the C-terminus could be capped as a 3° amide, thus reducing polarity and increasing membrane permeability. The methyl group (**39**) had the same affinity as the nonsubstituted amide (**3**). The benzyl group in peptide **40** results in somewhat higher affinity than that provided by threonine in peptide **2** (409 vs 739 nM). The differences between the benzyl (**40**) and the (*S*)-(**41**) and (*R*)-(**42**) methylbenzyl groups suggest that the aromatic groups are interacting with the protein and that the latter, more structured substituents somewhat impede the interaction. Thus, it seems likely that there is a hydrophobic surface on the Stat3 SH2 domain that accommodates the pY+4 region of the peptide inhibitor.



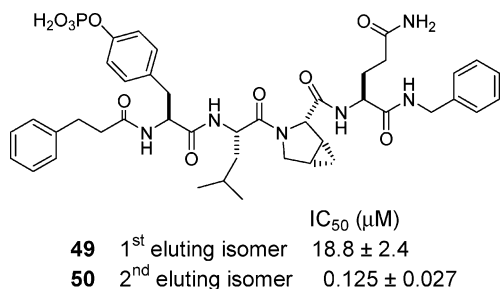


**Figure 2.** Structure and IC<sub>50</sub> values of PhCH<sub>2</sub>CH<sub>2</sub>CO-Tyr(OPO<sub>3</sub>H<sub>2</sub>)-Leu-3,4-*cis*-methanoPro-Gln-NHBn.

The low affinities of the disubstituted amide analogues suggest that the C-terminal amide bond is a hydrogen bond donor. That replacing Gln with Gaba, which does not possess that carboxamide group, results in lower affinity is in keeping with important inter- or intramolecular interactions involving the Gln backbone carboxamide. *N*-Methylthreonine resulted in a slight loss in activity; IC<sub>50</sub> is 1.2 μM for peptide **48** versus 0.74 μM for peptide **2**.

#### Development of a High-Affinity Tetrapeptide.

A peptide was synthesized that incorporated the amino acids that produced the highest affinity at each position: hydrocinnamoyl on the N-terminus, *cis*-3,4-methanoproline at pY+2, and benzyl at pY+4 (Figure 2). As in peptides **18** and **19**, two diastereomers were isolated by preparative HPLC: **49** and **50**. In this case the order of affinity was reversed, the first eluting isomer, **49**, had an IC<sub>50</sub> of 18.8 ± 2.4 μM. However, the second isomer, **50**, was a highly potent inhibitor with an IC<sub>50</sub> of 0.125 ± 0.027 μM, 6-fold more active than pentapeptide **2**, the lead peptide for this paper, and 2.3-fold more active than the original hexapeptide peptide lead **1**. The hydrophobic dihydrocinnamoyl group on the N-terminus, the methanoPro, and the C-terminal benzylamide resulted in additive effects on affinity.

#### Conclusions

Our results suggest that a hydrogen bond exists between the αNH of Leu at pY+1 of our peptides and the C=O of Ser 636 of Stat3 as seen in the crystal structure.<sup>29</sup> Thus, we are confident the Tyr(PO<sub>3</sub>H<sub>2</sub>)-Leu part of our lead peptide binds to Stat3 in a "standard" manner for phosphopeptide/SH2 domain complexes (Figure 1). There appears to be a hydrophobic surface on Stat3 that binds pY-1 substituents. *cis*-3,4-Methanoproline was the optimum scaffold at position pY+2. The stereochemistry of the enantiomer that produces the high affinity is not known. Whether the methano group makes important binding contact with Stat3 or causes a conformational effect is unclear and is under investigation. Glutamine at position pY+3 is very important for affinity. Attempts to replace the side chain amide protons with methyl groups or to replace the amide nitrogen with a methyl group (Met(O)) were deleterious, suggesting a hydrogen-bonding role. The lower affinity of the larger methyl-substituted amide suggests a tight fit of the CONH<sub>2</sub> into a binding pocket on the surface of Stat3. The intact structure of glutamine is optimal. Removal of the α-carboxyl group resulted in a loss of activity, suggesting a role for this group in restriction of rotation of the bulk of the residue or a role in hydrogen binding. Slight increases in activity of

benzyl and (*S*)-α-methylbenzyl groups suggest a hydrophobic binding pocket for the pY+4 residue. With the exception of 3-carboxamidoaniline, constrained cyclic Gln mimics showed modest losses in activity. Thus, it may be possible to constrain the CONH<sub>2</sub> group to a conformation close to that of the bound peptide.

The purpose of these studies was to gain information for the development of peptidomimetic inhibitors of Stat3. Our results suggest that the design of such compounds should include the aryl phosphate, the α-NH of pY+1, an intact side chain CONH<sub>2</sub> at pY+3, and N- and C-terminal hydrophobic groups. That peptide **50**, containing these features, was higher in affinity than our lead peptide **1** confirms our conclusions.

#### Experimental Section

N<sup>α</sup>-Protected amino acids were purchased from Advanced Chemtech, NovaBiochem, ChemImpex, or AnaSpec. HOBt was from ChemImpex. Rink amide resin was from Advanced Chemtech, loaded between 0.6 and 0.7 mmol/g. PL-DMA, a polydimethylacrylamide-based resin, was purchased from Polymer Laboratories, Ltd. Anhydrous DMF for amino acid solutions was from Baker. Other solvents were reagent grade and were used without further purification.

Peptides were purified by reverse-phase HPLC on a Rainin rabbit HPLC using a Vydac 2.5 cm × 25 cm C18 peptide and protein column. Gradients of ACN in H<sub>2</sub>O (both containing 0.1% TFA) or MeOH or ACN in 0.01 M NH<sub>4</sub>OAc (pH 6.5) at 10 mL/min were employed. Peptides were tested for purity by reverse-phase HPLC on a Hewlett-Packard 1090 HPLC or an Agilent 1100 HPLC using a Vydac 4.6 mm × 250 mm C18 peptide/protein column in two systems, one with 0.1% TFA in both H<sub>2</sub>O and ACN (systems A–C) and the other with increasing gradients of ACN or MeOH in 0.01 M NH<sub>4</sub>OAc, pH 6.5 (systems D–G).

A	0–40% ACN (0.1%TFA)
B	10–50% ACN (0.1%TFA)
C	10–80% ACN (0.1%TFA)
D	5–45% MeOH in 0.01 M NH <sub>4</sub> OAc, pH 6.5
E	15–55% MeOH in 0.01 M NH <sub>4</sub> OAc, pH 6.5
F	5–45% ACN in 0.01 M NH <sub>4</sub> OAc, pH 6.5
G	15–55% ACN in 0.01 M NH <sub>4</sub> OAc, pH 6.5

All gradients were run at 1.5 mL/min and detection at 230 and 275 nm was performed simultaneously.

**Fluorescence Polarization Assays.** A 50 μL aliquot of a solution of 0.8 μg of full length Stat3α (160 nM) and 20 nM of probe in 50 mM NaCl, 10 mM Hepes, 1 mM Na<sub>2</sub>EDTA, 2 mM DTT, and 1% NP-40 was placed in wells of a 96-well microtiter plate. To each well was added 50 μL of a peptide solution in the same buffer. Fluorescence polarization was then read in a Tecan Polarizer plate reader. With use of Prizm, version 4, from GraphPad Software, Inc., the mP was plotted against the log of the peptide concentration and IC<sub>50</sub> values were obtained from non-linear regression analysis in the one-site competition mode. Peptides were assayed three times using three separate Stat3-probe preparations. IC<sub>50</sub> values are reported as the mean of three IC<sub>50</sub> values ± the standard deviation. Full length Stat3 was a gift from Dr. Xiaomin Chen.

**Solid-Phase Peptide Synthesis: Automated Method.** Individual reactor vessels on an Advanced Chemtech 348 multiple peptide synthesizer were charged with 0.200 g of Rink amide resin. Amino acids were dissolved to a concentration of 0.4 M in DMF containing 0.4 M HOBt. For coupling, 2 mL of amino acid solution and 2 mL of 0.4 M DIPCPI (in CH<sub>2</sub>Cl<sub>2</sub>) were transferred to the resin, and the mixture was vortexed for 1 h. The resin was drained and washed 5× with 4.5 mL of DMF/CH<sub>2</sub>Cl<sub>2</sub>. Fmoc removal was accomplished with two treatments of 4.5 mL of 20% piperidine in DMF for 5 and 10 min each. Resins were washed 5× with DMF/CH<sub>2</sub>Cl<sub>2</sub>. Cleavage was accomplished with three treatments of the resins with 5 mL

of TFA/TIS/H<sub>2</sub>O (95:2.5:2.5)<sup>34</sup> for 10 min each. The combined filtrates sat at room temperature for 2 h. The volumes of the solvents were reduced, and the solutions were dropped into ice-cold Et<sub>2</sub>O. After 30 min, the precipitates were collected by filtration and were washed 2× more with Et<sub>2</sub>O. Crude peptides were dried, and peptides were purified by reverse-phase HPLC. All peptides were dried over P<sub>2</sub>O<sub>5</sub> in vacuo at 37 °C, and peptide contents were calculated from the absorbance at 268 nM using the extinction coefficient  $\epsilon = 695 \text{ M}^{-1} \text{ cm}^{-1}$ .<sup>46</sup> Peptide yields, HPLC retention times, and mass spectra are tabulated in the Supporting Information.

**Solid-Phase Peptide Synthesis: Manual Method.** Manual solid-phase synthesis was carried out on aliquots of 0.20 g of Rink resin (0.6 mmol/g) or Rink-handle derivatized PL-DMA resin. Fmoc groups were removed with 2 × 5 mL of 20% piperidine for 3 and 7 min each. For coupling, 3-fold excesses of Fmoc-amino acids, PyBop, and HOBt were used along with 6-fold excesses of DIPEA in 4 mL of DMF/CH<sub>2</sub>Cl<sub>2</sub>. After coupling and deprotection steps, resins were washed with 3 × 5 mL of DMF/CH<sub>2</sub>Cl<sub>2</sub>. For the introduction of phosphotyrosine, Fmoc-Tyr(PO[NMe<sub>2</sub>]<sub>2</sub>)-OH was used. Cleavage was accomplished with three treatments of the resins with 5 mL of TFA/TIS/H<sub>2</sub>O (95:2.5:2.5)<sup>34</sup> for 10 min each. The filtrates were combined. After 2 h, 3 mL of H<sub>2</sub>O was added and the reaction sat at room temperature overnight. The volumes of the solvents were reduced, and the solutions were dropped into ice-cold Et<sub>2</sub>O. After 30 min the precipitates were collected by filtration and were washed 2× more with Et<sub>2</sub>O. Crude peptides were dried, and peptides were purified by reverse-phase HPLC. All peptides were dried over P<sub>2</sub>O<sub>5</sub> in vacuo at 37 °C, and peptide contents were calculated from the absorbance at 268 nM using the extinction coefficient  $\epsilon = 695$ . Peptide yields, HPLC retention times, and mass spectra are tabulated in Table 1.

**Preparation of PL-DMA Resin.** Polydimethylacrylamide-based PL-DMA resin was treated overnight with neat ethylenediamine as described in Arshady et al.<sup>49</sup> After thoroughly washing the resin with DMF/CH<sub>2</sub>Cl<sub>2</sub>, Fmoc-Rink linker was added in 3-fold excess, as calculated from the nominal loading of 1 mmol/g. Coupling was mediated with 3-fold excesses of PyBOP, HOBt, and a 6-fold excess of DIEA. On completion of the coupling as judged by negative ninhydrin tests, the resin was drained, washed with DMF/CH<sub>2</sub>Cl<sub>2</sub> and CH<sub>2</sub>Cl<sub>2</sub>, and then dried under vacuum and stored.

**Solid-Phase Synthesis of Peptides 27, 28, 39–47.** These peptides were synthesized in parallel on aliquots of 0.20 g of Rink amide resin (0.6 mmol/g, 0.12 mmol) on an Advanced Chemtech 348 multiple synthesizer employing a 40-well reactor block. For peptides **27** and **28**, the sequence Ac-Tyr(PO[NMe<sub>2</sub>]<sub>2</sub>)-Leu-Pro-Glu(OAll)-Thr(<sup>t</sup>Bu) (**51**) was synthesized in two wells. For peptides **39–47**, the sequence Ac-Tyr(PO[NMe<sub>2</sub>]<sub>2</sub>)-Leu-Pro-Gln-OAll (**55**) was synthesized in 10 wells. Note that the latter peptide was attached to the resin via the side chain of the C-terminal Gln by using Fmoc-Glu-OAll. On completion of the syntheses, the resins were washed with 5 × 4.5 mL of CH<sub>2</sub>Cl<sub>2</sub>. A solution of 30 mM Pd[PPh<sub>3</sub>]<sub>4</sub> in CHCl<sub>3</sub>/AcOH/NMM (37:2:1), 4 mL, was added to each well by syringe using the automated synthesizer. The reactor was rotated for 2 h. The resin was drained and then washed with 5 × 4 mL of DMF/CH<sub>2</sub>Cl<sub>2</sub>, 3 × 4 mL of 2% Na<sub>2</sub>S<sub>2</sub>CNMe<sub>2</sub> in DMF, 3 × 4 mL of 0.5% HOBt in DMF, then 5 × 4 mL of DMF/CH<sub>2</sub>Cl<sub>2</sub>. Resins were then derivatized in parallel as follows.

**Ac-Tyr(PO<sub>3</sub>H<sub>2</sub>)-Leu-Pro-Gln(Me)-Thr-NH<sub>2</sub>, 27.** A solution of 0.6 mmol each of MeNH<sub>3</sub>Cl, PyBOP, and HOBt plus 1.2 mmol of DIEA in 4 mL of DMF was added to resin-bound Ac-Tyr(PO[NMe<sub>2</sub>]<sub>2</sub>)-Leu-Pro-Glu-Thr(<sup>t</sup>Bu) in one reactor well. After 5 h the resin was drained and washed with DMF/CH<sub>2</sub>Cl<sub>2</sub> followed by CH<sub>2</sub>Cl<sub>2</sub>. The peptide was cleaved with 3 × 5 mL of TFA/TIS/H<sub>2</sub>O (95:2.5:2.5) for 10 min each. The combined cleavage solutions were mixed with 1.5 mL of H<sub>2</sub>O, and the solution sat overnight. The TFA volume was reduced, and the residue was dropped into ice-cold Et<sub>2</sub>O to precipitate the product. After the peptide was washed in Et<sub>2</sub>O, it was purified by reverse-phase HPLC using a gradient of MeOH in 0.01M

NH<sub>4</sub>OAc and purified to give 47.1 mg of peptide. HPLC *t*<sub>R</sub> (A–D) 12.63; ESI-MS (M + H) calcd 756.75, found 756.5.

**Ac-pTyr-Leu-Pro-Gln(Me<sub>2</sub>)-Thr-NH<sub>2</sub>, 28.** Synthesized as per **27** except that dimethylamine was coupled to the glutamic acid side chain. Yield 31.1 mg. HPLC *t*<sub>R</sub> (A–D) 14.17; ESI-MS (M + H) calcd 770.78, found 770.5.

**Ac-Tyr(PO<sub>3</sub>H<sub>2</sub>)-Leu-Pro-Gln-NHMe, 39.** Resin-bound Ac-Tyr(PO[NMe<sub>2</sub>]<sub>2</sub>)-Leu-Pro-Gln-OH was treated with 0.6 mmol each of MeNH<sub>3</sub>Cl, DIPCDI, and HOBt in DMF/CH<sub>2</sub>Cl<sub>2</sub> plus 0.6 mmol of DIEA in 4 mL of DMF/CH<sub>2</sub>Cl<sub>2</sub>. After 5 h the resin was drained and washed with DMF/CH<sub>2</sub>Cl<sub>2</sub> followed by CH<sub>2</sub>Cl<sub>2</sub>. The peptide was cleaved and purified as described above for **27**. Yield 30.3 mg. HPLC *t*<sub>R</sub> (A) 13.05, (D) 12.16; ESI-MS (M + H) calcd 655.28, found 655.4. Peptides **40–49** were synthesized as per **39** using the appropriate base.

**Synthesis of Ac-Tyr(PO<sub>3</sub>H<sub>2</sub>)-Leu-Pro-3-carboxamidobenzamide, 33.** Boc-proline (0.869 g, 4.04 mmol), 3-aminobenzamide (0.500 g, 3.67 mmol), HBTU (1.39 g, 3.67 mmol), and DBU (1.10 mL, 7.34 mmol) were stirred in 7 mL of DMF overnight. The solvent was removed in vacuo, and the residue was taken up in EtOAc and washed with 2% KHSO<sub>4</sub>, 5% NaHCO<sub>3</sub>, and brine. After drying (MgSO<sub>4</sub>) and evaporation, the yield was 0.621 g (1.94 mmol, 53%). The residue was stirred in TFA for 1 h, and the acid was removed in vacuo. Toluene was added and evaporated off twice to remove excess TFA. The residue was stirred in 7 mL of DMF/CH<sub>2</sub>Cl<sub>2</sub> (1:1). Boc-Leu-OH (0.492 g, 1.95 mmol), EDC (0.378 g, 1.95 mmol), and NMM (0.214 mL, 1.95 mmol) were added, and the mixture stirred overnight. The solvents were removed in vacuo, and the residue was taken up in EtOAc and washed as before. After the mixture was dried (MgSO<sub>4</sub>), the solvent was removed to yield 0.866 g of a white solid (1.94 mmol, 100%). The product was treated with 20 mL of TFA for 1 h, precipitated in Et<sub>2</sub>O, collected by centrifugation, and washed with Et<sub>2</sub>O twice more. After the mixture was dried, the yield was 0.478 g (1.04 mmol, 53%). To 0.300 g (0.652 mmol) of residue in 5 mL of DMF/CH<sub>2</sub>Cl<sub>2</sub> (1:1) was added 0.385 g of Fmoc-Tyr(PO[NMe<sub>2</sub>]<sub>2</sub>)-OH (0.716 mmol), 0.137 g of EDC (0.716 mmol), and 0.079 mL of NMM (0.716 mmol). After overnight reaction, 0.160 mL of NMM was added and the reaction allowed to proceed overnight. The solvents were removed in vacuo, and the residue was taken up in 30 mL of EtOAc. The organic phase was washed with acid and base as before, dried, and evaporated to yield 0.150 g of an off-white powder. This residue was stirred in 1 mL of 2% DBU in DMF for 1 h. Ac<sub>2</sub>O, 40 μL, was added, and after 2 h the product was precipitated by the addition of Et<sub>2</sub>O. It was collected by centrifugation and washed with Et<sub>2</sub>O. The product was treated with 3 mL of 90% (aqueous) TFA overnight, precipitated in Et<sub>2</sub>O, centrifuged, and washed with Et<sub>2</sub>O. After purification by reverse-phase HPLC, the yield was 19.1 mg. HPLC *t*<sub>R</sub> (A) 18.01, (D) 24.88; ESI-MS (M + H) calcd 695.31, found 695.3.

**Synthesis of (R,S)-Fmoc-pyrrolidine-3-acetic Acid, 58.** To 20 mL of 1:1 acetone/H<sub>2</sub>O was added pyrrolidine-3-acetic acid (1.0 g, 6.88 mmol), Fmoc-OSu (2.3 g, 6.88 mmol), and NaHCO<sub>3</sub> (2.19 g, 20.6 mmol), and the solution was stirred overnight. The acetone was removed by evaporation in vacuo, and the water layer was extracted with 3 × 15 mL of ethyl acetate. The organic extracts were pooled, dried over MgSO<sub>4</sub>, and filtered, and the solvent was evaporated in vacuo to yield 1.69 g (4.82 mmol, 70% yield) of a white solid. HPLC *t*<sub>R</sub> (A) 6.453; ESI-MS (M + 1) calcd 353.15, found 353.3; <sup>1</sup>H NMR (300 MHz, CDCl<sub>3</sub>)  $\delta$  7.76 (d, 2H, *J* = 7.35 Hz), 7.60 (d, 2H, *J* = 7.54 Hz), 7.39 (tr, 2H, *J* = 7.34 Hz), 7.31 (tr, 2H, *J* = 7.53 Hz), 4.40 (m, 2H), 4.24 (m, 1H), 3.73 (m, 1H, C(2)H<sub>a</sub>), 3.54 (m, 1H, C(5)H<sub>a</sub>), 3.40 (m, 1H, C(5)H<sub>b</sub>), 3.09 (m, 1H, C(2)H<sub>b</sub>), 2.63 (m, 1H, C(3)H), 2.48 (m, 2H, exoCH<sub>2</sub>), 2.16 (m, 1H, C(4)H<sub>a</sub>), 1.64 (m, 1H, C(4)H<sub>b</sub>); <sup>13</sup>C NMR (75 MHz, CDCl<sub>3</sub>)  $\delta$  (176.60, 176.34, doublet), 154.91, 144.10, 141.34, 127.67, 127.02, 125.10, 119.96, 67.64 (51.67, 51.32, doublet), 47.76 (45.93, 45.65, doublet), 37.446 (35.75, 34.67, doublet), 31.89 and 31.10 (doublet).

**Synthesis of Fmoc-Glu-NH-Bn, 59.** Fmoc-glutamic acid  $\gamma$ -*tert*-butyl ester (1.00 g, 2.26 mmol) was stirred in 20 mL of



ACN along with 0.520 g of 1-ethyl-3-(3-dimethylaminopropyl)-carbodiimide hydrochloride (2.71 mmol), 191.7 g of HOBt (2.71 mmol), and 0.247 mL of benzylamine (2.26 mmol). After overnight reaction, the solvent was removed in vacuo and the residue was taken up in 100 mL of EtOAc. The organic solution was washed with 2% KHSO<sub>4</sub>, 5% NaHCO<sub>3</sub>, and brine. After the mixture was dried (MgSO<sub>4</sub>) and filtered, the solvent was removed to give a white solid. The residue was treated with 30 mL of TFA/H<sub>2</sub>O (95:5) for 1 h, and the solvent was removed in vacuo. Toluene was added and evaporated 2× to give 1.10 g of a white powder (100% yield), which was used without further purification: mp 178–180; <sup>1</sup>H NMR (300 MHz, DMSO-*d*<sub>6</sub>) δ 8.38 (tr, 1H, NHBn), 7.89 (d, 2H, Fmoc arom, *J* = 7.4 Hz), 7.74 (d, 2H, Fmoc arom, *J* = 6.4 Hz), 7.57 (d, 1H, Gln NH, *J* = 8.1 Hz), 7.2–7.4 (m, 9H Fmoc, Bn arom), 4.2 (m, 5H, Fmoc CH–CH<sub>2</sub>, Bn CH<sub>2</sub>), 4.06 (m, 1H, Glu αCH), 2.28 (br tr, 2H, Glu γCH<sub>2</sub>), 1.97 (m, 1H Glu βCH) 1.83 (m, 1H, Glu βCH); <sup>13</sup>C NMR (75.5 MHz) δ 174.72, 172.35, 156.87, 144.77, 144.63, 141.58, 140.24, 129.08, 128.50, 127.94, 127.58, 126.18, 120.96, 66.57, 55.00, 47.55, 42.95, 41.21, 31.17, 28.12, 21.60.

**Acknowledgment.** We are grateful to the National Cancer Institute for support of this work (Grant CA096652). We also acknowledge the NCI Cancer Center Support Grant CA016672 for the support of our NMR facility and both the M. D. Anderson Cancer Center Proteomics Facility and the Structural Biology Program for mass spectrometry.

**Supporting Information Available:** Tables of compound characterization and <sup>1</sup>H NMR assignments for peptides 1–3. This material is available free of charge via the Internet at <http://pubs.acs.org>.

## References

- (1) (a) Bromberg, J.; Darnell, J. E., Jr. The role of STATs in transcriptional control and their impact on cellular function. *Oncogene* **2000**, *19*, 2468–2473. (b) Levy, D. E.; Darnell, J. E., Jr. Stats: transcriptional control and biological impact. *Nat. Rev. Mol. Cell Biol.* **2002**, *3*, 651–662. (c) Stark, G. R.; Kerr, I. M.; Williams, B. R.; Silverman, R. H.; Schreiber, R. D. How cells respond to interferons. *Annu. Rev. Biochem.* **1998**, *67*, 227–264.
- (2) Akira, S.; Nishio, Y.; Inoue, M.; Wang, X. J.; Wei, S.; Matsusaka, T.; Yoshida, K.; Sudo, T.; Naruto, M.; Kishimoto, T. Molecular cloning of APRF, a novel IFN-stimulated gene factor 3 p91-related transcription factor involved in the gp130-mediated signaling pathway. *Cell* **1994**, *77*, 63–71.
- (3) (a) Zhong, Z.; Wen, Z.; Darnell, J. E., Jr. Stat3: A STAT family member activated by tyrosine phosphorylation in response to epidermal growth factor and interleukin-6. *Science* **1994**, *264*, 95–98. (b) Zhong, Z.; Wen, Z.; Darnell, J. E., Jr. Stat3 and Stat4: Members of the Family of signal transducers and activators of transcription. *Proc. Nat. Acad. Sci. U.S.A.* **1994**, *91*, 4806–4810.
- (4) Stahl, N.; Farruggella, T. J.; Boulton, T. G.; Zhong, Z.; Darnell, J. E.; Yancopoulos, G. D. Choice of STATs and other substrates specified by modular tyrosine-based motifs in cytokine receptors. *Science* **1995**, *267*, 1349–1353.
- (5) Gerhartz, C.; Heesel, B.; Sasse, J.; Hemmann, U.; Landgraf, C.; Schneider-Mergener, J.; Horn, F.; Heinrich, P. C.; Graeve, L. Differential activation of acute phase response factor/STAT3 and STAT1 via the cytoplasmic domain of the interleukin 6 signal transducer gp130. I. Definition of a novel phosphotyrosine motif mediating STAT1 activation. *J. Biol. Chem.* **1996**, *271*, 12991–12998.
- (6) (a) Coffey, P.; Kruijer, W. EGF receptor deletions define a region specifically mediating STAT transcription factor activation. *Biochem. Biophys. Res. Commun.* **1995**, *210*, 74–81. (b) Tong, Z.; Jing, M.; Xinmin, C. Grb2 regulates Stat3 activation negatively in epidermal growth factor signalling. *Biochem. J.* **2003**, *376*, 457–464.
- (7) Schreiner, S. J.; Schiavone, A. P.; Smithgall, T. E. Activation of STAT3 by the Src family kinase Hck requires a functional SH3 domain. *J. Biol. Chem.* **2002**, *277*, 45680–45687.
- (8) Song, J. I.; Grandis, J. R. STAT signaling in head and neck cancer. *Oncogene* **2000**, *19*, 2489–2495.
- (9) Garcia, R.; Yu, C. L.; Hudnall, A.; Catlett, R.; Nelson, K. L.; Smithgall, T.; Fujita, D. J.; Ethier, S. P.; Jove, R. Constitutive activation of Stat3 in fibroblasts transformed by diverse oncoproteins and in breast carcinoma cells. *Cell Growth Differ.* **1997**, *8*, 1267–1276.
- (10) Schaefer, L. K.; Ren, Z.; Fuller, G. N.; Schaefer, T. S. Constitutive activation of Stat3a in brain tumors: localization to tumor endothelial cells and activation by the endothelial tyrosine kinase receptor (VEGFR-2). *Oncogene* **2002**, *21*, 2058–2065.
- (11) Dhir, R.; Ni, Z.; Lou, W.; DeMiguel, F.; Grandis, J. R.; Gao, A. C. Stat3 activation in prostatic carcinomas. *Prostate* **2002**, *51*, 241–246.
- (12) Seki, Y.; Suzuki, N.; Imaizumi, M.; Iwamoto, T.; Usami, N.; Ueda, Y.; Hamaguchi, M. STAT3 and MAPK in human lung cancer tissues and suppression of oncogenic growth by JAB and dominant negative STAT3. *Int. J. Oncol.* **2004**, *24*, 931–934.
- (13) Benekli, M.; Baer, M. R.; Baumann, H.; Wetzler, M. Signal transducer and activator of transcription proteins in leukemias. *Blood* **2003**, *101*, 2940–2954.
- (14) Catlett-Falcone, R.; Landowski, T. H.; Oshiro, M. M.; Turkson, J.; Levitzki, A.; Savino, R.; Ciliberto, G.; Moscinski, L.; Fernandez-Luna, J. L.; Nunez, G.; Dalton, W. S.; Jove, R. Constitutive activation of Stat3 signaling confers resistance to apoptosis in human U266 myeloma cells. *Immunity* **1999**, *10*, 105–115.
- (15) Weber-Nordt, R. M.; Egen, C.; Wehinger, J.; Ludwig, W.; Gouilleux-Gruart, V.; Mertelsmann, R.; Finke, J. Constitutive activation of STAT proteins in primary lymphoid and myeloid leukemia cells and in Epstein–Barr virus (EBV)-related lymphoma cell lines. *Blood* **1996**, *88*, 809–816.
- (16) Scholz, A.; Heinze, S.; Detjen, K. M.; Peters, M.; Welzel, M.; Hauff, P.; Schirner, M.; Wiedenmann, B.; Rosewicz, S. Activated signal transducer and activator of transcription 3 (STAT3) supports the malignant phenotype of human pancreatic cancer. *Gastroenterology* **2003**, *125*, 891–905.
- (17) (a) Bowman, T.; Garcia, R.; Turkson, J.; Jove, R. STATs in oncogenesis. *Oncogene* **2000**, *19*, 2474–2488. (b) Buettner, R.; Mora, L. B.; Jove, R. Activated STAT signaling in human tumors provides novel molecular targets for therapeutic intervention. *Clin. Cancer Res.* **2002**, *8*, 945–954. (c) Bromberg, J. Stat proteins and oncogenesis. *J. Clin. Invest.* **2002**, *109*, 1139–1142. (d) Darnell, J. E., Jr. Transcription factors as targets for cancer therapy. *Nat. Rev. Cancer* **2002**, *2*, 740–749. (e) Yu, H.; Jove, R. The STATs of cancer. New molecular targets come of age. *Nat. Rev. Cancer* **2004**, *4*, 97–105.
- (18) (a) Burke, W. M.; Jin, X.; Lin, H.-J.; Huang, M.; Liu, R.; Reynolds, R. K.; Lin, J. Inhibition of constitutively active Stat3 suppresses growth of human ovarian and breast cancer cells. *Oncogene* **2001**, *20*, 7925–7934. (b) Niu, G.; Heller, R.; Catlett-Falcone, R.; Coppola, D.; Jaroszeski, M.; Dalton, W.; Jove, R.; Yu, H. Gene therapy with dominant-negative Stat3 suppresses growth of the murine melanoma B16 tumor in vivo. *Cancer Res.* **1999**, *59*, 5059–5063. (c) Grandis, J. R.; Drenning, S. D.; Chakraborty, A.; Zhou, M.-Y.; Zeng, Q.; Pitt, A. S.; Tweardy, D. J. Requirement of Stat3 but not Stat1 activation for epidermal growth factor receptor-mediated cell growth in vitro. *J. Clin. Invest.* **1998**, *102*, 1385–1392. (d) Grandis, J. R.; Drenning, S. D.; Zeng, Q.; Watkins, S. C.; Melhem, M. F.; Endo, S.; Johnson, D. E.; Huang, L.; He, Y.; Kim, J. D. Constitutive activation of Stat3 signaling abrogates apoptosis in squamous cell carcinogenesis in vivo. *Proc. Natl. Acad. Sci. U.S.A.* **2000**, *97*, 4227–4232.
- (19) Real, P. J.; Sierra, A.; de Juan, A.; Segovia, J. C.; Lopez-Vega, J. M.; Fernandez-Luna, J. L. Resistance to chemotherapy via Stat3-dependent overexpression of Bcl-2 in metastatic breast cancer cells. *Oncogene* **2002**, *21*, 7611–7618.
- (20) Garcia, R.; Bowman, T. L.; Niu, G.; Yu, H.; Minton, S.; Muro-Cacho, C. A.; Cox, C. E.; Falcone, R.; Fairclough, R.; Parsons, S.; Laudano, A.; Gazit, A.; Levitzki, A.; Kraker, A.; Jove, R. Constitutive activation of Stat3 by the Src and JAK tyrosine kinases participates in growth regulation of human breast carcinoma cells. *Oncogene* **2001**, *20*, 249–2513.
- (21) (a) Sawyer, T. K. Src homology-2 domains: structure, mechanisms, and drug discovery. *Biopolymers* **1998**, *47*, 243–261. (b) Cody, W. L.; Lin, Z.; Panek, R. L.; Rose, D. W.; Rubin, J. R. Progress in the development of inhibitors of SH2 domains. *Curr. Pharm. Des.* **2000**, *6*, 59–98. (c) Muller, G. Peptidomimetic SH2 domain antagonists for targeting signal transduction. *Top. Curr. Chem.* **2001**, *211*, 17–59. (d) Shakespeare, W. C. SH2 domain inhibition: a problem solved? *Curr. Opin. Chem. Biol.* **2001**, *5*, 409–415. (e) Metcalf, C. A., III; Sawyer, T. Src Homology-2 Domains and Structure-based, Small-molecule Library Approaches to Drug Discovery. In *Drug Discovery Strategies and Methods*; Makriyannis, A., Biegel, D., Eds.; Marcel Dekker: New York, 2004; pp 23–59.
- (22) Pawson, T. Protein modules and signalling networks. *Nature* **1995**, *373*, 573–580.
- (23) (a) Songyang, Z.; Shoelson, S. E.; Chaudhuri, M.; Gish, G.; Pawson, T.; Haser, W. G.; King, F.; Roberts, T.; Ratnofsky, S.; Lechleider, R. J. SH2 domains recognize specific phosphopeptide sequences. *Cell* **1993**, *72*, 767–778. (b) Songyang, Z.; Shoelson,

- S. E.; McGlade, J.; Olivier, P.; Pawson, T.; Bustelo, X. R.; Barbacid, M.; Sabe, H.; Hanafusa, H.; Yi, T. Specific motifs recognized by the SH2 domains of Csk, 3BP2, fps/fes, GRB-2, HCP, SHC, Syk, and Vav. *Mol. Cell. Biol.* **1994**, *14*, 2777–2785.
- (24) Park, O. K.; Schaefer, L. K.; Wang, W.; Schaefer, T. S. Dimer stability as a determinant of differential DNA binding activity of Stat3 isoforms. *J. Biol. Chem.* **2000**, *275*, 32244–32249.
- (25) Turkson, J.; Ryan, D.; Kim, J. S.; Zhang, Y.; Chen, Z.; Haura, E.; Laudano, A.; Sebt, S.; Hamilton, A. D.; Jove, R. Phosphotyrosyl peptides block Stat3-mediated DNA-binding activity, gene regulation and cell transformation. *J. Biol. Chem.* **2001**, *276*, 45443–45455.
- (26) Ren, Z.; Cabell, L. A.; Schaefer, T. S.; McMurray, J. S. Identification of a high affinity phosphopeptide inhibitor of Stat3. *Bioorg. Med. Chem. Lett.* **2003**, *13*, 633–636.
- (27) Shao, H.; Cheng, H. Y.; Cook, R. G.; Tweardy, D. J. Identification and characterization of signal transducer and activator of transcription 3 recruitment sites within the epidermal growth factor receptor. *Cancer Res.* **2003**, *63*, 3923–3930.
- (28) Waksman, G.; Schoelson, S. E.; Pant, N.; Cowburn, D.; Kuriyan, J. Binding of a high affinity phosphotyrosyl peptide to the Src SH2 domain: crystal structures of the complexed and peptide free forms. *Cell* **1993**, *72*, 779–790.
- (29) Becker, S.; Gromer, B.; Muller, C. W. Three-dimensional structure of the Stat3 $\beta$  homodimer bound to DNA. *Nature* **1998**, *394*, 145–151.
- (30) (a) Xu, R. X.; Word, J. M.; Davis, D. G.; Rink, M. J.; Willard, D. H., Jr.; Gampe, R. T., Jr. Solution structure of the human p60<sup>src</sup> SH2 domain complexed with a phosphorylated tyrosine pentapeptide. *Biochemistry* **1995**, *34*, 2107–2121. (b) Plumme, R. M. S.; Holland, D. R.; Shahripour, A.; Lunney, E. A.; Fergus, J. H.; Marks, J. S.; McConnell, P.; Mueller, W. T.; Sawyer, T. K. Design, synthesis, and cocrystal structure of a nonpeptide Src SH2 domain ligand. *J. Med. Chem.* **1997**, *40*, 3719–3725. (c) Ettmayer, P.; France, D.; Gounarides, J.; Jarosinski, M.; Martin, M. S.; Rondeau, J. M.; Sabio, M.; Topiol, S.; Weidmann, B.; Zurini, M.; Bair, K. W. Structural and conformational requirements for high-affinity binding to the SH2 domain of Grb2. *J. Med. Chem.* **1999**, *42*, 971–980 (d) Tong, L.; Warren, T. C.; King, J.; Betageri, R.; Rose, J.; Jakes, S. Crystal structures of the human p56<sup>lck</sup> SH2 domain in complex with two short phosphotyrosyl peptides at 1.0 Å and 1.8 Å resolution. *J. Mol. Biol.* **1996**, *256*, 601–610. (e) Breeze, A. L.; Kara, B. V.; Barratt, D. G.; Anderson, M.; Smith, J. C.; Luke, R. W.; Best, J. R.; Cartledge, S. A. Structure of a specific peptide complex of the carboxy-terminal SH2 domain from the p85 alpha subunit of phosphatidylinositol 3-kinase. *EMBO J.* **1996**, *15*, 3579–89. (f) Pauptit, R. A.; Dennis, C. A.; Derbyshire, D. J.; Breeze, A. L.; Weston, S. A.; Rowsell, S.; Murshudov, G. N. NMR trial models: experiences with the colicin immunity protein Im7 and the p85alpha C-terminal SH2-peptide complex. *Acta Crystallogr., Sect. D* **2001**, *57* (Part 10), 1397–1404.
- (31) (a) Chen, X.; Vinkemeier, U.; Zhao, Y.; Jeruzalmi, D.; Darnell, J. E.; Kuriyan, J. Crystal structure of a tyrosine phosphorylated STAT-1 dimer bound to DNA. *Cell* **1998**, *93*, 827–839. (b) Mao, X.; Ren, Z.; Parker, G. N.; Sondermann, H.; Pastorello, M. A.; Wang, W.; McMurray, J. S.; Demeler, B.; Darnell, J. E., Jr.; Chen, X. Structural bases of unphosphorylated STAT1 association and receptor binding. *Mol. Cell* **2005**, *17*, 761–771.
- (32) Parts of this work were published in a preliminary communication: Ren, Z.; Coleman, D. R.; Cabell, L. A.; McMurray, J. S. The Development of Peptide-Based Inhibitors of Stat3 $\alpha$ . In *Peptide Revolution: Genomics, Proteomics & Therapeutics*, Proceedings of the 18th American Peptide Symposium; Chorev, M., Sawyer, T. K., Eds.; American Peptide Society: San Diego, CA; 2004, pp 550–552.
- (33) Ottinger, E. A.; Shekels, L. L.; Bernlohr, D. A.; Barany, G. Synthesis of phosphotyrosine-containing peptides and their use as substrates for protein tyrosine phosphatases. *Biochemistry* **1993**, *32*, 4354–4361.
- (34) Pearson, D. A.; Blanchette, M.; Baker, M. L.; Guindon, C. A. Trialkylsilanes as scavengers for the trifluoroacetic acid de-blocking of protecting groups in peptide synthesis. *Tetrahedron Lett.* **1989**, *30*, 2739–2742.
- (35) Kates, S. A.; Daniels, S. B.; Albericio, F. Automated allyl cleavage for continuous-flow synthesis of cyclic and branched peptides. *Anal. Biochem.* **1993**, *212*, 303–310.
- (36) Chao, H.-G.; Bernatowicz, M. S.; Reiss, P. D.; Matsueda, G. R. Synthesis and application of bis-silylethyl-derived phosphate-protected Fmoc-phosphotyrosine derivatives for peptide synthesis. *J. Org. Chem.* **1994**, *59*, 6687–6691.
- (37) (a) Chao, H.-G.; Leiting, B.; Reiss, P. D.; Burkhardt, A. L.; Klimas, C. E.; Bolen, J. B.; Matseuda, G. R. Synthesis and Application of Fmoc-O-[bis(dimethylamino)phosphono]tyrosine, a versatile protected phosphotyrosine equivalent. *J. Org. Chem.* **1995**, *60*, 7710–7711. (b) Ueki, M.; Tachibana, J.; Ishii, Y.; Okumura, J.; Goto, M. *N,N'*-Dialkylamide-type phosphate protecting groups for Fmoc synthesis of phosphotyrosine-containing peptides. *Tetrahedron Lett.* **1996**, *37*, 4953–4956. (c) Ueki, M.; Goto, M.; Okumura, J.; Ishii, Y. *N,N'*-Dialkylamide-type phosphate protecting groups for Fmoc synthesis of phosphotyrosine-containing peptides: Optimization of the alkyl group. *Bull. Chem. Soc. Jpn.* **1998**, *71*, 1887–1898.
- (38) Chan, W. C.; Bycroft, B. W.; Evans, D. J.; White, P. D. A novel 4-aminobenzyl ester-based carboxy-protecting group for synthesis of atypical peptides by Fmoc-But solid-phase chemistry. *J. Chem. Soc., Chem. Commun.* **1995**, *21*, 2209–2210.
- (39) Haan, S.; Hemmann, U.; Hassiepen, U.; Schaper, F.; Schneider-Mergener, J.; Wollmer, A.; Heinrich, P. C.; Grotzinger, J. Characterization and binding specificity of the monomeric STAT3-SH2 domain. *J. Biol. Chem.* **1999**, *274*, 1342–1348.
- (40) (a) Lynch, B. A.; Loiacono, K. A.; Tiong, C. L.; Adams, S. E.; MacNeil, I. A. A fluorescence polarization based Src-SH2 binding assay. *Anal. Biochem.* **1997**, *247*, 77–82. (b) Wu, P.; Brasseur, M.; Schindler, U. A high-throughput STAT binding assay using fluorescence polarization. *Anal. Biochem.* **1997**, *249*, 29–36. (c) Schust, J.; Berg, T. A high-throughput fluorescence polarization assay for signal transducer and activator of transcription 3. *Anal. Biochem.* **2004**, *330*, 114–118.
- (41) Turkson, J.; Kim, J. S.; Zhang, S.; Yuan, J.; Huang, M.; Glenn, M.; Haura, E.; Sebt, S.; Hamilton, A. D.; Jove, R. Novel peptidomimetic inhibitors of signal transducer and activator of transcription 3 dimerization and biological activity. *Mol. Cancer Ther.* **2004**, *3*, 261–269.
- (42) Goodman, M.; Ro, S. Peptidomimetics for Drug Design. In *Burger's Medicinal Chemistry and Drug Discovery*, 5th ed.; Wolff, M. E., Ed.; John Wiley & Sons Inc.: New York, 1995; pp 803–861.
- (43) García-Echeverría, C.; Furet, P.; Gay, G.; Fretz, H.; Rahuel, J.; Schoepfer, J.; Caravatti, G. Potent antagonists of the SH2 domain of Grb2: Optimization of the X<sub>-1</sub> position of 3-amino-Z-Tyr(PO<sub>3</sub>H<sub>2</sub>)-X<sub>-1</sub>-Asn-NH<sub>2</sub>. *J. Med. Chem.* **1998**, *41*, 1741–1744.
- (44) (a) Chakraborty, A.; Dyer, K. F.; Cascio, M.; Mietzner, T. A.; Tweardy, D. J. Identification of a novel Stat3 recruitment and activation motif within the granulocyte colony-stimulating factor receptor. *Blood* **1999**, *93*, 15–24. (b) Weber-Nordt, R. M.; Riley, J. K.; Greenlund, A. C.; Moore, K. W.; Darnell, J. E.; Schreiber, B. D. Stat-3 recruitment by two distinct ligand-induced, tyrosine-phosphorylated docking sites in the interleukin-10 receptor intracellular domain. *J. Biol. Chem.* **1996a**, *271*, 27954–27961. (c) Coffey, P.; Kruijer, W. EGF receptor deletions define a region specifically mediating STAT transcription factor activation. *Biochem. Biophys. Res. Commun.* **1995**, *210*, 74–81.
- (45) Wiederkehr-Adam, M.; Ernst, P.; Muller, K.; Bieck, E.; Gombert, F. O.; Ottl, J.; Graff, P.; Grossmuller, F.; Heim, M. H. Characterization of phosphopeptide motifs specific for the Src homology 2 domains of signal transducer and activator of transcription 1 (STAT1) and STAT3. *J. Biol. Chem.* **2003**, *278*, 16117–16128.
- (46) Bradshaw, J. M.; Waksman, G. Calorimetric investigation of proton linkage by monitoring both the enthalpy and association constant of binding: application to the interaction of the Src SH2 domain with a high-affinity tyrosyl phosphopeptide. *Biochemistry* **1998**, *37*, 15400–15407.
- (47) Arshady, R.; Atherton, E.; Clive, D. L. J.; Sheppard, R. C. Peptide synthesis. Part 1. Preparation and use of polar supports based on polydimethylacrylamide. *J. Chem. Soc., Perkin Trans. 1* **1981**, 529–537.
- (48) DeLano, W. L. *The PyMOL Molecular Graphics System*; DeLano Scientific LLC: San Carlos, CA; <http://www.pymol.org>.